Journal of Crystal Growth 312 (2010) 1316–1320

Contents lists available at ScienceDirect

Journal of Crystal Growth

journal homepage: www.elsevier.com/locate/jcrysgro

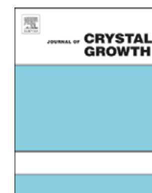

Crystal quality improvement of *a*-plane GaN using epitaxial lateral overgrowth on nanorods

Shih-Chun Ling [a,*], Chu-Li Chao [b,c], Jun-Rong Chen [a], Po-Chun Liu [b], Tsung-Shine Ko [a], Tien-Chang Lu [a,d], Hao-Chung Kuo [a], Shing-Chung Wang [a], Shun-Jen Cheng [c], Jenq-Dar Tsay [b]

[a] Department of Photonics and Institute of Electro-Optical Engineering, National Chiao Tung University, 1001 University Road, Hsinchu, Taiwan 300, ROC
[b] Electronics and Optoelectronics Research Laboratories, Industrial Technology Research Institute, 195 Chung Hsing Road, Section 4 Chu Tung, Hsinchu, Taiwan 310, ROC
[c] Department of Electrophysics, National Chiao Tung University, 1001 University Road, Hsinchu, Taiwan 300, ROC
[d] Institute of Lighting and Energy Photonics, National Chiao Tung University, 301 Gaofa 3rd Road, Guiren Township, Tainan, Taiwan 711, ROC

ARTICLE INFO

Available online 28 October 2009

Keywords:
A3. Metalorganic chemical vapor deposition
B1. Nitrides
B2. Semiconducting gallium compounds
A1. Characterization

ABSTRACT

The crystal quality of *a*-plane GaN films was improved by using epitaxial lateral overgrowth on nano-rod GaN template. The scanning electron microscope images showed the fully coalesced regrowth process completed within only 2 μm thickness. The *a*-plane GaN films grown on nano-rod template showed superior surface quality and less surface pits. The on-axis and off-axis FWHMs of X-ray rocking curves decreased with the increase in the etching depth of the nano-rod template. TEM analysis revealed that the dislocation density was reduced to around $1.2\times10^{9}\,cm^{-2}$ by the nano-rod epitaxial lateral overgrowth. In addition, the photoluminescence intensity of the *a*-plane GaN was enhanced significantly. These results demonstrated the opportunity of achieving *a*-plane GaN films with high crystal quality via nano-rod epitaxial lateral overgrowth.

© 2009 Elsevier B.V. All rights reserved.

1. Introduction

Nitride-based light-emitting diodes (LEDs) are attracting great attention for their potential applications in solid-state lighting. However, the conventional *c*-plane nitride-based quantum wells exhibit the quantum-confined stark effect as a result of the existence of spontaneous and piezoelectric polarization fields that are parallel to [0 0 0 1] *c*-direction [1,2]. This effect results in spatial separation of the electron and hole wave functions in the quantum wells, which restricts the carrier recombination efficiency, reduces oscillator strength, and induces red-shifted emission [3]. To avoid such polarization effects, growth along $[11\bar{2}0]$-oriented direction has been explored for planar *a*-plane GaN prepared on *r*-plane sapphire [4] and *a*-plane SiC [5] by metalorganic chemical vapor deposition (MOCVD). Since these GaN surfaces contain an equal number of Ga and N atoms in each monolayer, free electric field and nonpolar characteristic are obtained. The recent studies of *a*-plane AlGaN/GaN [6,7] and InGaN/GaN [8,9] multi-quantum wells (MQWs) demonstrate that it is possible to eliminate such polarization fields along the nonpolar orientation.

However, the difficult issue to utilize nonpolar GaN is that no suitable substrate can be used for hetero-epitaxial *a*-plane GaN growth. In general, a threading dislocation (TD) density of $\sim3\times10^{10}\,cm^{-2}$ and on-axis X-ray diffraction full width at half maximum (FWHM) of $\sim0.3^{\circ}$ were commonly observed in *a*-plane GaN grown on *r*-plane sapphire because of the large anisotropic lattice mismatch between these two materials [4]. The TDs in GaN act as nonradiative recombination centers and charge scattering centers which are responsible for poor internal quantum efficiency and low carrier mobilities [10,11]. Therefore, the reduction of TD density is essential to improve the performance of *a*-plane light-emitting devices. Lateral epitaxial overgrowth (LEO) techniques were widely employed in the past to reduce defect density in nonpolar GaN [12]. In our previous work, we performed the LEO on 0.5-μm-height nanorods with SiO_2 sidewall passivation to realize the defect reduction and quality improvement in the subsequently grown *a*-plane GaN layer [13]. The average TD density can be reduced from 3×10^{10} to $3.5\times10^{8}\,cm^{-2}$. The X-ray diffraction FWHMs for on- and off-axis reflections were also decreased from 1308 to 430 arcsec and from 2420 to 1148 arcsec, respectively. Although the quality improvement in *a*-plane GaN was apparently achieved via the special LEO technique, the full coalescence by this LEO technique requires more than 10 μm as a result of the difficulties in the uniformity of SiO_2 sidewall passivation. Therefore, in this study, the process step of SiO_2 sidewall passivation was skipped and a series of nano-rod templates with varied etching depth were developed to

* Corresponding author. Tel.: +886 3 5131234; fax: +886 3 5716631.
E-mail addresses: ginowell@hotmail.com (S.-C. Ling), timtclu@mail.nctu.edu.tw (T.-C. Lu), hckuo@faculty.nctu.edu.tw (H.-C. Kuo).

0022-0248/$ - see front matter © 2009 Elsevier B.V. All rights reserved.
doi:10.1016/j.jcrysgro.2009.10.047

optimize the quality improvement in the subsequently grown *a*-plane GaN layer. The newly developed nano-rod epitaxial lateral overgrowth (NRELOG) is more advantageous because of thin coalescence thickness (less than 2 μm), lower cost (no additional SiO_2 passivation), and ease to achieve high-quality *a*-plane GaN films.

2. Experimental details

The schematic flowchart of NRELOG is shown in Fig. 1. First, a 1.7-μm-thick *a*-plane GaN layer was grown on *r*-plane sapphire by MOCVD, followed by the deposition of a SiO_2 film with a 200 nm thickness and a Ni film with a 10 nm thickness acting as etching masks. Subsequently, a rapid thermal annealing treatment of 850 °C was utilized to obtain nano-scale Ni masks. Then, the GaN nanorods were etched through the nano-mask openings by reactive ion etching (RIE)/inductively coupled plasma etching (ICP). The etchants for RIE were SF_6 and Ar, and the etchants for ICP etching were Ar, BCl_3, and Cl_2. After that, the residual SiO_2 masks on nanorods were removed by hydrofluoric acid to simplify the growth process. The nanorods exhibit a random distribution with arbitrary geometries as shown in Fig. 2(a). The diameter of the nanorod is 300–500 nm and the nanorod density is estimated to be around $6\times10^8 cm^{-2}$. In order to optimize the quality improvement in the regrown *a*-plane GaN layer, we designed a series of nano-rod templates with different etching depths (t) from 0.2 to 1.7 μm. Finally, the GaN regrowth was performed by MOCVD on these nano-rod templates. The growth temperature, pressure, and V/III ratio were 1180 °C, 200 mbar, and 800–900, respectively.

3. Results and discussion

Fig. 2(b) shows the scanning electron microscope (SEM) images of initial regrowth on *a*-plane GaN nanorods at a 45° angle of view. After 10 min of MOCVD regrowth, the nanorods, which at first exhibited a random distribution, were aligned along the *c*-direction. In cross-sectional SEM view as shown in Fig. 2(c), the Ga-face sidewalls of the nanorods formed arrowhead-like shapes with inclined $\{11\bar{2}n\}$ facets since the growth rate on the Ga-face (+*c*-direction) was about 10 times higher than that on the N-face (–*c*-direction) [12]. The N-face became the straight side-wall and maintained mirror-like flatness. The Ga-face sidewalls gradually combined with the N-face facets and finally became a fully coalesced GaN film. As shown in Fig. 2(d), the NRELOG coalesced process can be completed within the thickness of 2 μm, which is thinner than that of the previous LEO approach (10 μm) [13]. In the fully coalesced GaN film, there are lots of voids left behind, which should be attributed to the extinction of precursor species during the combination of Ga- and N-face sidewalls. Fig. 3 shows the 3×3 μm^2 atomic force microscope (AFM) images of (a) as-grown sample and NRELOG samples with nanorod etching depths of (b) 0.5 μm, (c) 1 μm, and (d) 1.4 μm, respectively. These samples were grown under the same growth conditions (the growth temperature, pressure, and V/III ratio were 1180 °C, 200 mbar, and 800–900, respectively). Compared with the as-grown sample, the NRELOG samples had superior surface quality and less surface pits. It is believed that surface pits originate from threading dislocation terminations at the surface [4]. Therefore, the fewer surface pits hints at the possibility that the density of dislocations was reduced. The roughness rms of the NRELOG sample with 1.4 μm etching depth was approximately 1.4 nm, which was smaller than that of the as-grown sample (nearly 4.1 nm).

A high resolution X-ray diffractometer (Bede D1) with a Cu target was employed to investigate the crystalline quality of GaN epilayers. All data are collected at 40 kV, 50 mA using a line focus X-ray source with 10 arcsec per step. The omega X-ray rocking curves (XRCs) for on-axis $(11\bar{2}0)$ and off-axis $(1\bar{1}01)$, $(11\bar{2}2)$ reflections for *a*-plane GaN films grown on the nano-rod templates with varied etching depth were measured. The XRC full width at half maximum (FWHM) of the GaN peaks are plotted in Fig. 4. The on-axis FWHMs of $\psi=0^\circ$ and $\psi=90^\circ$ (*c*- and *m*-mosaic, respectively) for as-grown GaN were 900 and 1480 arcsec, respectively. The off-axis $(1\bar{1}01)$, $(11\bar{2}2)$ peaks, which measure the twist mosaics, were 2420 and 1680 arcsec, respectively. It is obvious that the on-axis and off-axis FWHMs for all reflections decreased with the increase in the etching depth of the nano-rod template. Also, it can been seen that for on-axis scans, the ratio of *m*-mosaic to *c*-mosaic approach unity with the increase in the etching depth of the nano-rod template. The minimum XRC FWHM values were obtained for the *a*-plane GaN film regrown on 1.7-μm-height nanorods. The on-axis FWHMs were 560 and 514 arcsec for $\psi=0^\circ$ and $\psi=90^\circ$ and the off-axis FWHMs were 1232 and 846 arcsec for $(1\bar{1}01)$ and $(11\bar{2}2)$ reflections. This decrease may signify the crystal quality improvement in the regrown *a*-plane GaN films.

Factors affecting the broadening of XRC FWHMs in nonpolar GaN, in addition to defect densities, may also include surface roughness effects, mosaic tilt, and wafer curvature [14]. Therefore, to precisely quantify the decrease in defect densities, transmission electron microscopy (TEM) analysis must be carried out. Fig. 5 shows the typical bright-field plan-view TEM images (acceleration voltage=120 kV) of the *a*-plane GaN film regrown on 1.7-μm-height nanorods. Fig. 5(a) was imaged under the g=0002 diffraction condition, revealing the TDs having a nonzero [0 0 0 1] Burgers vector component. The TD density of the NRELOG sample with 1.7 μm etching depth was estimated to be around 1.2×10^9 cm^{-2}, a 1–2 order of magnitude lower than that of the as-grown sample. Fig. 5(b), taken under the $g=10\bar{1}0$ diffraction condition, shows a stacking fault (SF) density of $\sim2\times10^5$ cm^{-1}, a 2-fold reduction relative to the as-grown sample.

The room temperature photoluminescence (PL) was enhanced with the increase in the etching depth of the nano-rod template as shown in Fig. 6. The maximum PL integrated intensity for the NRELOG GaN has a 19-fold increase compared to that of the as-grown GaN. TEM results have revealed that the stacking fault

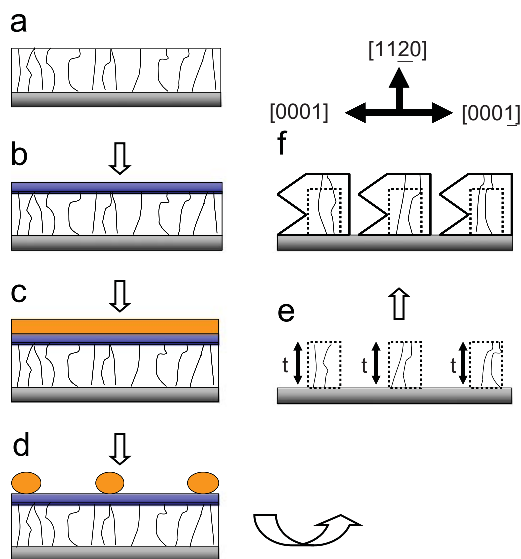

Fig. 1. Flowchart of *a*-plane GaN NRELOG process.

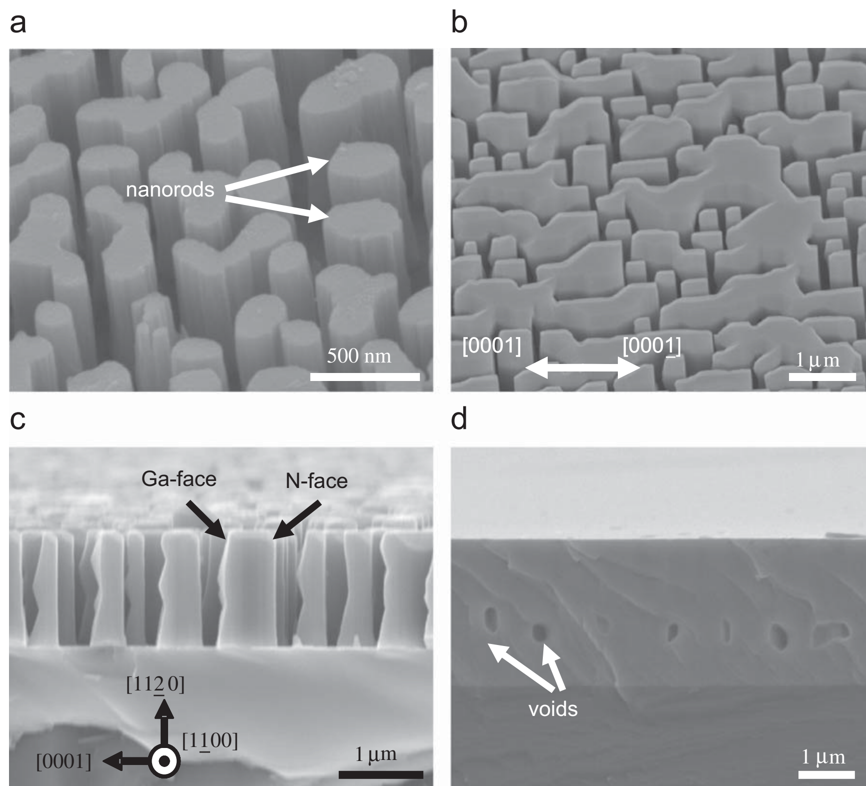

Fig. 2. SEM images of (a) fabricated GaN nanorods; (b) initial MOCVD regrowth on *a*-plane GaN nanorods at a 45° angle of view and (c) at a 90° angle of view; (d) fully coalesced *a*-plane GaN films in cross-sectional view.

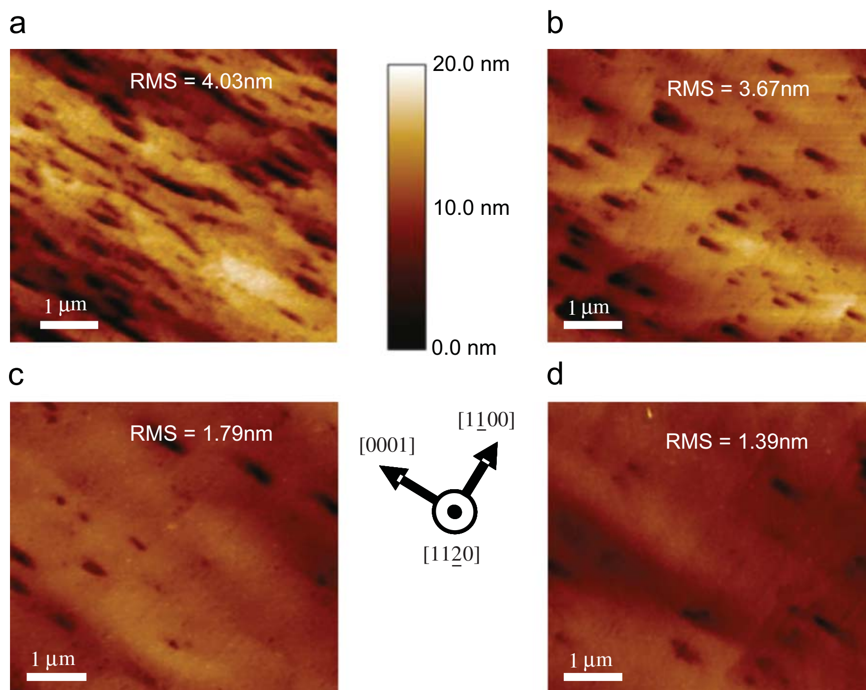

Fig. 3. AFM images (3 × 3 μm^2) of (a) as-grown sample and *a*-plane GaN films grown on the nano-rod templates with (b) 0.5 μm etching depth, (c) 1 μm etching depth, and (d) 1.4 μm etching depth, respectively.

density in the NRELOG sample was decreased by a factor of 2 compared to that of the as-grown sample. Since the intensity of basal plane stacking fault (BSF) emission correlates with the stacking fault density in *a*-plane GaN, the intensity of BSF-related emission contributing to near band-edge emission must decrease in NRELOG samples. Therefore, the 19-fold increase of the PL intensity for the NRELOG sample could be attributed to the significant reduction in dislocation density in the NRELOG GaN film, which has been proven by the TEM image (Fig. 5(a)). Since the density of nonradiative recombination centers was reduced, the

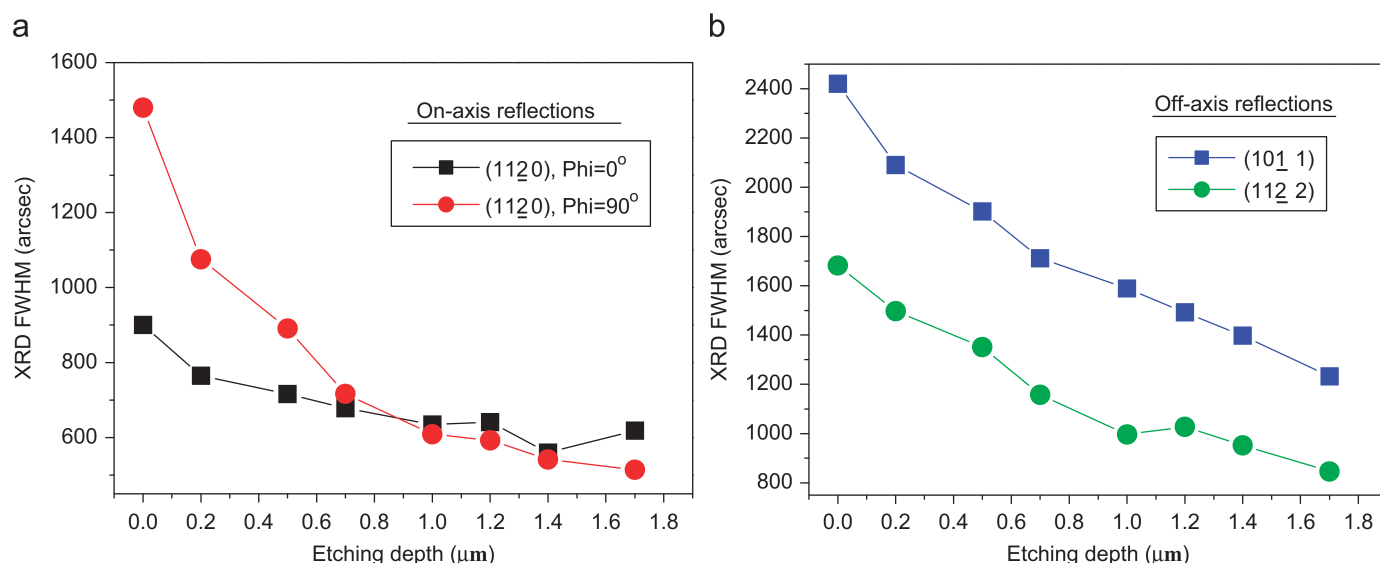

Fig. 4. (a) On-axis and (b) off-axis XRC FWHMs of *a*-plane GaN films grown on the nano-rod templates with varied etching depth.

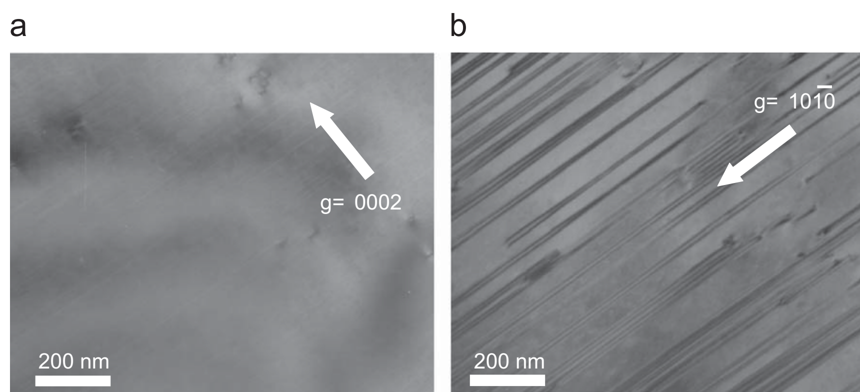

Fig. 5. Plan-view TEM images of the *a*-plane GaN film regrown on 1.7-μm-height nanorods as observed with (a) g=0002 to observe dislocations having a nonzero [0 0 0 1] component and (b) $g = 10\bar{1}0$ to observe stacking faults parallel to the (0 0 0 1) plane.

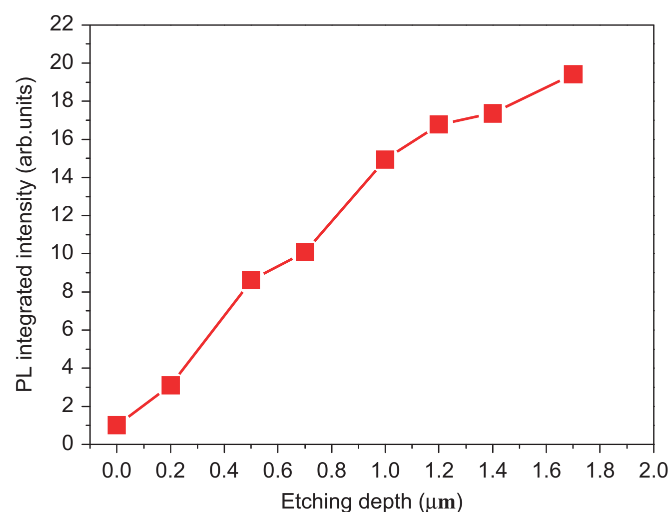

Fig. 6. Improvement of GaN band-edge PL emission for *a*-plane GaN films grown on the nano-rod templates with varied etching depth.

intensity of GaN-related emission should be enhanced. However, a partial PL enhancement may be attributed to the increase in light extraction as a result of residual voids in NRELOG samples.

4. Conclusion

In summary, we have grown high-quality and fully coalesced *a*-plane GaN films by using NRELOG. The fully coalesced thickness of NRELOG sample was decreased to only 2 μm. The use of NRELOG resulted in the reduction of on-axis and off-axis XRC FWHMs and also resulted in superior surface quality and less surface pits in *a*-plane GaN films. TEM images also showed that the TD density of the NRELOG sample was reduced to about 1.2×10^9 cm^{-2}, which is a 1–2 order of magnitude decrease as compared to that of the as-grown sample. Moreover, the intensity of GaN band-edge luminescence was enhanced, which could be attributed to the decrease in TD density. A series of experiments demonstrated the feasibility of using the NRELOG technique to achieve crystal quality improvement in *a*-plane GaN grown on *r*-plane sapphire.

Acknowledgements

This work was supported by the Ministry of Economic Affairs of the Republic of China (MOEA) and in part by the National Science Council of Taiwan under Contract no. NSC 96-2221-E009-094-MY3. The number of the MOEA project was 7301XS1G20 for the nonpolar GaN epitaxy and MOVPE part.

References

[1] T. Takeuchi, S. Sota, M. Katsuragawa, M. Komori, H. Takeuchi, H. Amano, I. Akasaki, Jpn. J. Appl. Phys. 36 (1997) 382.
[2] D.A.B. Miller, D.C. Chemla, T.C. Damen, A.C. Grossard, W. Wiegmann, T.H. Wood, C.A. Burrus, Phys. Rev. B 32 (1985) 1043.
[3] J.S. Im, H. Kollmer, J. Off, A. Sohmer, F. Scholz, A. Hangleiter, Phys. Rev. B 57 (1998) 9435.
[4] M.D. Craven, S.H. Lim, F. Wu, J.S. Speck, S.P. DenBaars, Appl. Phys. Lett. 81 (2002) 469.
[5] M.D. Craven, A. Chakraborty, B. Imer, F. Wu, S. Keller, U.K. Mishra, J.S. Speck, S.P. DenBaars, Phys. Status Solidi C 1 (2003) 4.
[6] G.A. Garrett, H. Shen, M. Wraback, B. Imer, B. Haskell, J.S. Speck, S. Keller, S. Nakamura, S.P. DenBaarsPhys. Status Solidi A 202 (2005) 846.
[7] H.M. Ng, Appl. Phys. Lett. 80 (2002) 4369.
[8] A. Chakraborty, B.A. Haskell, S. Keller, J.S. Speck, S.P. DenBaars, S. Nakamura, U.K. Mishra, Appl. Phys. Lett. 85 (2004) 5143.
[9] A. Chakraborty, S. Keller, C. Meier, B.A. Haskell, S. Keller, P. Waltereit, S.P. DenBaars, S. Nakamura, J.S. Speck, U.K. Mishra, Appl. Phys. Lett. 86 (2005) 031901.
[10] H.M. Ng, D. Doppalapudi, T.D. Moustakas, N.G. Weimann, L.F. Eastman, Appl. Phys. Lett. 73 (2005) 821.
[11] N.G. Weimanna, L.F. Eastman, D. Doppalapudi, H.M. Ng, T.D. Moustakas, J. Appl. Phys. 83 (1998) 3656.
[12] B.A. Haskell, F. Wu, M.D. Craven, S. Matsuda, P.T. Fini, T. Fujii, K. Fujito, S.P. DenBaars, J.S. Speck, S. Nakamura, Appl. Phys. Lett. 83 (2003) 644.
[13] S.C. Ling, C.L. Chao, J.R. Chen, P.C. Liu, T.S. Ko, T.C. Lu, H.C. Kuo, S.C. Wang, S.J. Cheng, J.D. Tsay, Appl. Phys. Lett. 94 (2009) 251912.
[14] M.A. Moram, C.F. Johnston, J.L. Hollander, M.J. Kappers, C.J. Humphreys, J. Appl. Phys. 105 (2009) 113501.